Progress In Electromagnetics Research B, Vol. 27, 307–325, 2011

DESIGN, IMPLEMENTATION AND PERFORMANCE OF ULTRA-WIDEBAND TEXTILE ANTENNA

Mai A. R. Osman, M. K. A. Rahim, M. Azfar N. A. Samsuri, F. Zubir, and K. Kamardin

Department of Radio Communication Engineering
Faculty of Electrical Engineering
Universiti Teknologi Malaysia, UTM JB 81310, Johor, Malaysia

Abstract—Communication technology is increasingly pervading everyday life. The rapid progress in wireless communication besides the increasing interest in wearable antennas and electronics in civil, medical, sport wear and military domains promises to replace wired-communication networks in the near future in which antennas are in more important role. Recently, there has been growing interest in the antenna community to merge between wearable systems technology, Ultra-Wideband (UWB) technology and textile technology. All these together have resulted in demand for flexible fabric antennas, which can be easily attached to a piece of clothing. In this paper, three different structures of UWB antennas using clothing materials and suitable for wearable application were fabricated and presented. The substrate of the designed antennas was made from jeans textile material, while radiating element and ground plane are made out of copper tape. The operating frequency of all three designs is between 3 GHz and 12 GHz. Measured results are compared with simulations and good agreement was observed.

1. INTRODUCTION

Utilization of textile materials for the development of flexible wearable systems has been rapid due to the recent miniaturization of wireless devices. As wearable computing is developing, there is an increasing need for a wireless wearable system with antennas playing a decisive role. For flexible antennas, textile materials form interesting substrates, because fabric antennas can be easily integrated into

Received 20 October 2010, Accepted 21 December 2010, Scheduled 23 December 2010
Corresponding author: Mohamad Kamal A. Rahim (mkamal@fke.utm.my).

clothes [1–3]. Conversely, UWB transmission devices do not need to transmit a high-power signal to the receiver and can have a longer battery life or be smaller to reduce the wearable devices size [4–11]. Several antennas have been developed for wearable antennas in the form of flexible metal patches on textile substrates [11–15]. By merging the UWB technology with wearable textile technology, three different structures of UWB antenna with partial ground plane were fabricated and presented in this paper. The substrate of the designed antennas was made from jeans textile material while the radiating element and ground plane are made from copper tape.

2. WEARABLE MATERIALS CONCERNS

Textile materials that are used as an antenna's substrates can be divided into two main categories, natural and man-made fibers. Synthetic fibers are an interesting subcategory of man-made fibers being polymers from their molecular structure.

On the other hand, textile materials generally have a very low dielectric constant, which reduces the surface wave losses and improves the impedance bandwidth of the antenna [1–3, 11–15]. In comparison with high dielectric substrates, textile antennas are physically larger. However, several wearable antennas aspects contribute in the overall design features of the antennas. These aspects can be concluded as follows:

Elastic properties of textile materials: The variation of dimensions due to stretching and compression are typical for fabrics. The changes in the resonant length of the antenna detune its frequency band while the substrate thickness changes the resonant frequency as well as the input impedance bandwidth. Hence, it is challenging to design a fabric antenna that has stable electrical characteristics without having any influence on the electromagnetic characteristics of the antenna. Thus, avoiding types of elastic fabrics might be the best choice for wearable textile materials.

Wetness: Water has much high dielectric constant than does the fabric. When a fabric antenna absorbs water, the moisture changes the antenna performance parameters dramatically. The higher dielectric constant of water dominates the antenna performance by reducing the resonant frequency. Since fabric antennas are used near the skin, the aspect of wetness of fabric due to human sweat becomes more important. In addition, wearable systems can be mounted on top of jackets or suits where the aspects of wetness raised up due to rain or washing the textile materials. Thus, wearable textile antenna designers need to put the wetness aspects in considerations when designing these

types of antennas [14, 15].

Bending: In general, wearable systems with flat antenna surfaces cannot be provided especially when antennas embedded within clothing in positions such as sleeves where bending is expected to occur. Bending could affect the resonance length of antennas; therefore, antennas should properly function in such conditions [14].

Vicinity of human body: Wearable antennas need to be designed to operate properly in the vicinity of human body. In addition, special attention must be paid to the Specific Absorption Rates (SAR), which aids in the quantitative study of power absorption issues required to meet the standards in order to avoid harm to human body. Thus, in the vicinity of the human body, several issues should be considered such as antenna input-match performance, radiation characteristics of the antenna, and the power absorbed in the human body [14].

Human body movements: local scattering plays a part in communications when human body movement is considered. Hence, human body is subject to many small movements even when standing, sitting, during normal activities, and even during playing of sports. Thus, significant variations in the channel could occur due to changes in the geometry of the body. In such conditions, characterization of radio-wave propagation needs to account both for the variable positioning of the antennas on the body, and variations in the channel due to body movements [15].

Currently, in this manuscript, the substrate of the designed antennas was made from jeans fabric, which is a kind of 100% cotton material. In addition, jeans fabric has been chosen considering the thickness and the elastic properties of the fabric in order to avoid any kind of variation in dimensions due to material stretching and compression. Three different structures have been designed and analyzed. In order to model the fabric it is important to know its relative permittivity. The measured relative permittivity for jeans fabric using the free space method at several frequencies was Approximately 1.7, while the conductive parts are made out of copper tape. These mentioned features together made the antenna flexible in nature. Table 1 illustrates the fabric thickness and the measured relative permittivity of jeans substrate textile material.

3. UWB ANTENNA DESIGN CONSIDERATION

Kinds of handful basic modifications were made on a previous published UWB antenna design reported in [1] in order to obtain this manuscript of UWB textile antenna design. In this paper, three

Table 1. Fabric thickness and measured relative permittivity of jeans substrate textile material by implementing the free space method.

Material	Values
Thickness, h [mm]	1
Measured relative permittivity, ε_r	1.7
Loss Tangent	0.025

different structures have been designed and analyzed, Circular UWB antenna with small radius (Antenna #1), Circular UWB antenna with large radius (Antenna #2), and Circular UWB antenna with centre hole (Antenna #3). In order to obtain these designs, few parameters needed to be calculated such as the radius of the radiating element. These parameters were calculated according to Equation (1):

$$a = \frac{87.94}{f_r\sqrt{\varepsilon_r}} \tag{1}$$

where a is the radius of the circular patch antenna in millimeter, f_r is the resonance frequency in GHz and ε_r is the relative permittivity of the textile substrate material.

Moreover, in order to accomplish all three designs presented in this manuscript, a partial ground plane was implemented in all antenna designs. Such types of truncated ground plane play an important role in the broadband and wideband characteristics of the designed antennas. In particular, this process can be related to the fact that ground plane truncation acts as an impedance matching element that controls the impedance bandwidth of the circular patch. Thus, it creates a capacitive load that neutralizes the inductive nature of the patch to produce nearly pure resistive input impedance [16–18].

4. MODELLING AND FABRICATION OF THE ANTENNAS

The conductive surfaces and the ground plane of all three designed antennas are made out of copper tape with a thickness of 0.03 mm. The simulations were carried out using CST Microwave Studio software and the fabric antennas characteristics were studied. Figure 1 below demonstrates CST Model of all three-antenna designs presented in this manuscript showing that the design of those antennas have been conducted in air space.

A 50 ohm microstrip feed line was provided for the antenna feed; hence the position was determined according to [19]. In addition,

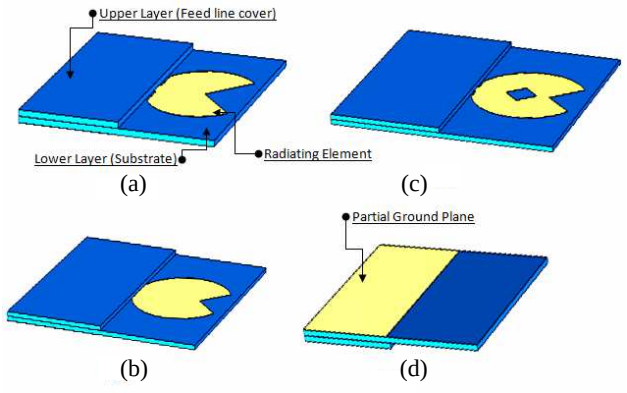

Figure 1. CST Simulation design models. (a) Top view of antenna #1. (b) Top view of antenna #2. (c) Top view of antenna #3. (d) Back view of partial ground plane.

authors of this manuscript planned to cover the feed line of all antenna designs by another layer of jeans fabric. The reason behind this, that those antennas were intended to be mounted or embedded in a wearable jacket or suit. Thus covering the feed line can provide a better out looking for all designed antennas. Moreover, the wearer would have more confident with a feeling that people around could not notice that an antenna exists in his/her clothes. According to that, a second layer of jeans fabric was placed on the top of the microstrip feed line with an air gap of 1 mm thickness. This air gap was implemented in the simulation part as well as fabrication process. All three different antenna structures were discussed in details as follows:

4.1. Antenna #1: Circular UWB Wearable Antenna with Small Radius

The first design is a basic modification of a previous published design reported in [1]. As in [1], the radiating element has a radius of 11 mm and a partial ground plane size of 36 mm $\times$ 20 mm. In addition, the substrate dimensions of antenna design mentioned in [1] was approximately 36 mm $\times$ 40 mm with a thickness of almost 1.5 mm. the overall thickness of this design mentioned in [1] was approximately 8.7 mm due to implementation of other materials such as dielectric materials and metallic disc used to ease the attachment of the button structure. As a Comparison to the present manuscript design, the radiating element of antenna #1 has a radius of 11 mm with one slit at

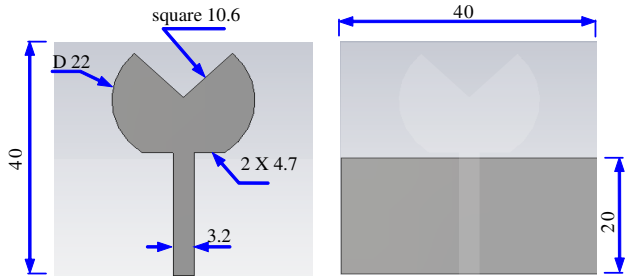

Figure 2. Dimensions in millimeters of Antenna #1 with both front and back views.

Table 2. Three different antenna prototypes and their dimensions in millimeters.

	Patch radius [mm]	Substrate dimensions [mm]	Partial ground plane dimensions [mm]	Air gap [mm]	Over all thickness	Centre Square slot dimensions [mm]
Antenna #1	11	40 × 40	40 × 20	1	2.6	-
Antenna #2	15	60 × 60	60 × 29	1	2.6	-
Antenna #3	15	60 × 60	50 × 29	1	2.6	6 × 6
Antenna mentioned in [1]	11	36 × 40	36 × 20	-	8.7	-

the top of the circular patch and two slits at the bottom of the circular patch. However, the jeans fabric substrate dimension is 40 mm × 40 mm with a partial ground plane size of 20 mm × 40 mm. Therefore, antenna designs presented in this paper give the impression of being more compact and easy to be mounted anywhere on the wearer clothes especially when compared with the original design mentioned in [1]. Figure 2 shows the dimensions of antenna #1, while Table 2 illustrates these dimensions as well as a comparison between the dimensions of all antennas presented in this manuscript and antenna design mentioned in [1].

4.2. Antenna #2: Circular UWB Wearable Antenna with Large Radius

A few modifications were made on the first design (Antenna #1) in order to obtain the second antenna design (Antenna #2). The dimension of the substrate is 60 mm × 60 mm, while the radius of the patch is 15 mm. In addition, a partial ground plane was made with a size of 60 mm × 29 mm, besides few changes in the dimensions of the upper and lower slits compared to antenna #1 slits size. Yet, all these dimensions are shown in Figure 3 and illustrated in Table 2.

4.3. Antenna #3: Circular UWB Wearable Antenna with Center Hole

Figure 4 shows the geometry and dimensions of both front and back views of the third and final antenna design (Antenna #3). The size of

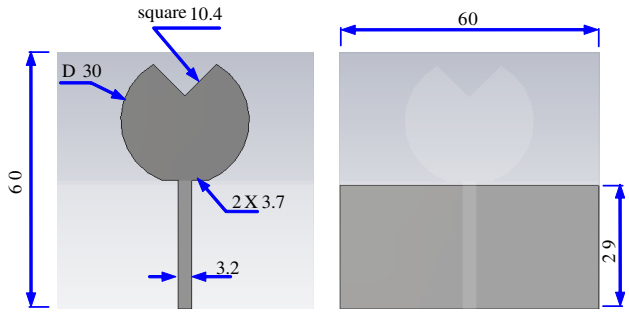

Figure 3. Dimensions in millimeters of Antenna #2 with both front and back views.

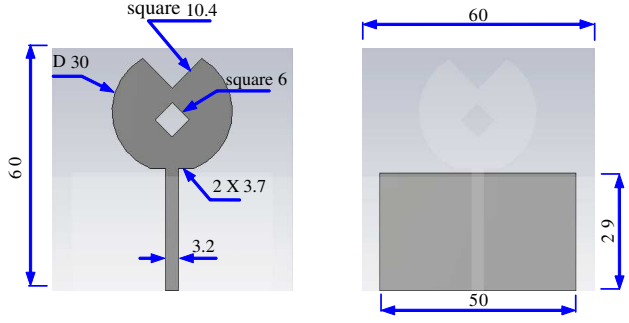

Figure 4. Dimensions in millimeters of Antenna #3 with both front and back views.

the substrate is 60 mm × 60 mm with a patch radius of 15 mm, which is similar to the design of antenna #2. In addition, the dimensions of the upper and lower slits remained the same compared to the design of antenna #2. The main difference between the design of antenna #3 and the previous two designs (antenna #1 and antenna #2) was achieved by creating a rotated square hole (slot) at the center of the circular patch with a size of 6 mm × 6 mm. The ground plane is a kind of a partial ground plane with a size of 50 mm × 29 mm. Yet, all theses dimensions are shown in Figure 4 and illustrated in Table 2.

Moreover, Figure 5 below demonstrates the geometry of three antennas prototypes mounted on the surface of jeans textile substrate material.

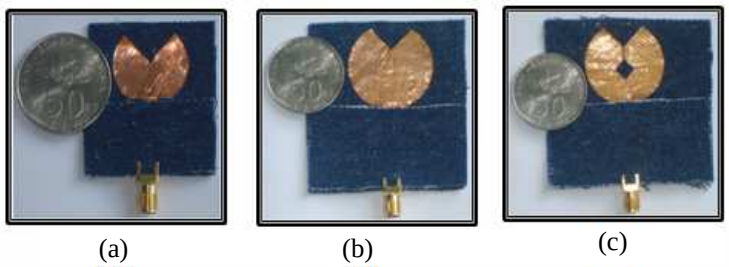

Figure 5. UWB Antenna Prototypes. (a) Antenna #1, UWB Wearable antenna with small radius. (b) Antenna #2, UWB wearable antenna with large radius. (c) Antenna #3, UWB wearable antenna with centre hole.

5. RESULTS AND DISCUSSIONS

In order to provide better investigation, this section will present a comparison of the simulated and measured return loss results as well as bandwidth results for all three antenna designs mentioned in the previous section. In addition, simulated results of radiation patterns, gain, efficiency, and current distribution of all three-antenna designs were also presented in this paper. Furthermore, the measured radiation pattern results of antenna #1 were also discussed in this manuscript to provide validation to results.

5.1. Return Loss Results

Authors of this manuscript compared earlier in previous sections of this paper between antenna #1 design and antenna design reported in [1] in terms of dimensions and design specifications. Thus in this

section, Discussions of the results will be initiated by comparing both simulated and measured results in terms of return loss and bandwidth for all three antenna designs, followed by return loss and bandwidth results discussion involving all three UWB antenna designs and original antenna design mention in [1].

Thus, in order to characterize all three designs of UWB antennas a network analyzer was used to measure the input return loss of the antennas as a function of frequency. Figure 6 demonstrates a snapshot of return loss measurement environment for all designs.

5.1.1. S_{11} Results of Antenna #1

Figure 7 below shows a comparison of both simulated and measured results in terms of return loss and bandwidth of antenna #1 design. The black solid line demonstrates the simulated results, while the blue dotted line shows the measured results. The measured results showed that it does agree very well with simulations and a wideband range of frequencies between 3 GHz and 12 GHz was covered by this design.

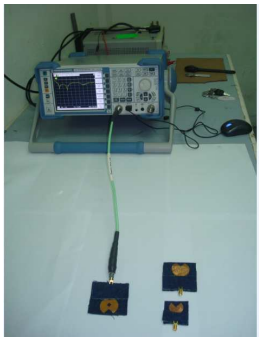

Figure 6. Snapshot of return loss and bandwidth measurement environment.

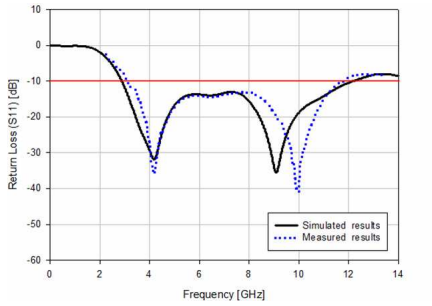

Figure 7. Simulated and measured return loss results of antenna #1 design.

5.1.2. S_{11} Results of Antenna #2

Conversely, similar comparisons between simulated and measured results for both return loss and bandwidth performance were made for antenna #2 design that is shown in Figure 8. The black solid line represents the simulated return loss and bandwidth results, while the blue dotted line shows the measured return loss and bandwidth results. From Figure 8, the measured results showed that it does agree very well

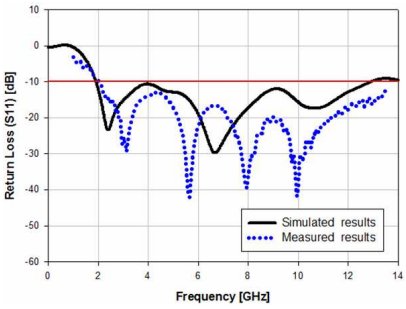

Figure 8. Simulated and Measured Return Loss results of antenna #2 design.

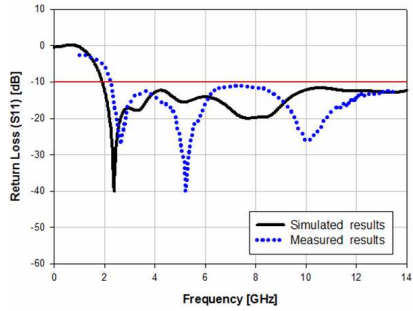

Figure 9. Simulated and measured return loss results of antenna #3 design.

with simulations and a wideband range of frequencies between 2 GHz and 13.5 GHz was covered by this design. Thus, results demonstrated that antenna #2 design had a wider bandwidth compared to antenna #1 design and even the antenna design reported in [1].

5.1.3. S_{11} Results of Antenna #3

In contrast, antenna #3 design has the widest band range of frequencies compared to the two previous designs presented in this manuscript. The black solid line shows the simulated return loss and bandwidth results, while the blue dotted line shows the measured return loss and bandwidth results. Figure 9 verified that the measured results agree very well with simulations, hence the simulated frequency range results is between 2 GHz and 14 GHz while the measured frequency range results is between 2 GHz and 13.5 GHz due to range limitation of the network analyzer used to measure those antennas.

5.1.4. S_{11} Results of Antenna Reported in [1]

However, in the case of antenna design stated in [1], the calculated and measured return loss and bandwidth result achieved was more than 3 GHz to 12 GHz with good agreement between the simulated and measured results. Since the results accomplished by all three UWB antenna designs of this manuscript was almost similar to antenna design reported in [1], even though the thickness of both designs was unalike, one can consider that all three antenna designs presented in this manuscript has made a step forward towards compactness.

5.2. Current Distribution Results

5.2.1. Current Results of Antenna #1

Current distribution determines how the current flows on the patch of the antenna. Figure 10 demonstrates these results of antenna #1 design with four different points of frequencies at 3 GHz, 5 GHz, 7 GHz, and 10 GHz. From Figure 10, one can observe that high strength of current radiates along the transmission line and the boundary of the patch. However, the boundary of the partial ground plane was also found to be a significant radiating area.

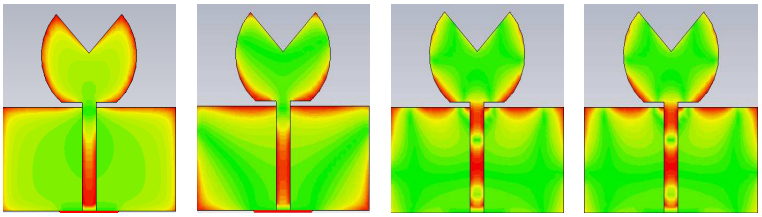

(a) 3 GHz (b) 5 GHz (c) 7 GHz (d) 10 GHz

Figure 10. Current flow simulated results of antenna #1 design.

5.2.2. Current Results of Antenna #2

In addition, Figure 11 demonstrates the results showing the current distributionof antenna #2 design with four different points of frequencies. As in Figure 11, current distribution results were almost similar to antenna #1 design, since high strength of current radiates along the transmission line and the boundary of the patch. However, the boundary of partial ground plane was also found to be a significant radiating area.

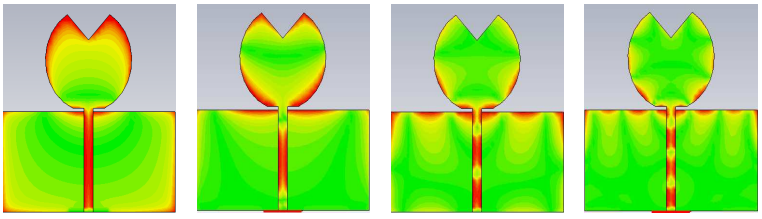

(a) 3 GHz (b) 5 GHz (c) 7 GHz (d) 10 GHz

Figure 11. Simulated current flow results of antenna #2 design.

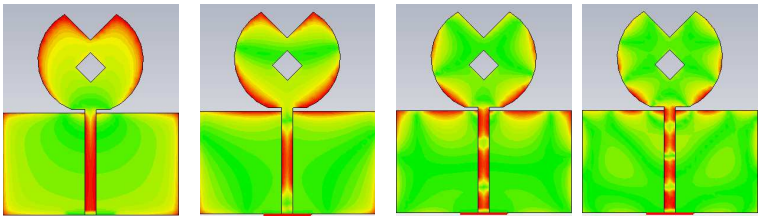

(a) 3 GHz (b) 5 GHz (c) 7 GHz (d) 10 GHz

Figure 12. Simulated current flow results of antenna #3 design.

5.2.3. Current Results of Antenna #3

In opposition, current distribution results of antenna #3 design were all demonstrated in Figure 12 with four different points of frequencies. As illustrated in Figure 12, the results were slightly different from the two previous designs, hence antenna #3 design has resulted in greater bandwidth. Besides that, the boundary of partial ground plane was also found to be a significant radiating area.

5.3. Radiation Pattern Results

A detailed discussion for the simulated results of radiation patterns of all three UWB antenna designs will be illustrated. After that, it will be followed by radiation pattern results discussion involving the original antenna design stated in [1]. Finally, the measured radiation pattern results of antenna #1 design will be covered at the end of this section.

5.3.1. Antenna #1 Polar Plot of Simulation Results

Figure 13 shows the behavior of 2D radiation pattern of E-plane and H-plane of antenna #1 design in the range of frequencies between 3 GHz and 10 GHz. At low frequencies, the radiation patterns of the antenna are almost alike. The pattern in E-plane resembles ring shape, while in H-plane the pattern resembles Omni-directional shape.

5.3.2. Antenna #2 Polar Plot of Simulation Results

Moreover, Figure 14 shows the behavior of 2D radiation pattern of E-plane and H-plane of antenna #2 design in the range of frequencies between 3 GHz and 10 GHz. At 3 GHz, most of signal intensity was found to be at the bottom of the antenna, while at 5 GHz most of

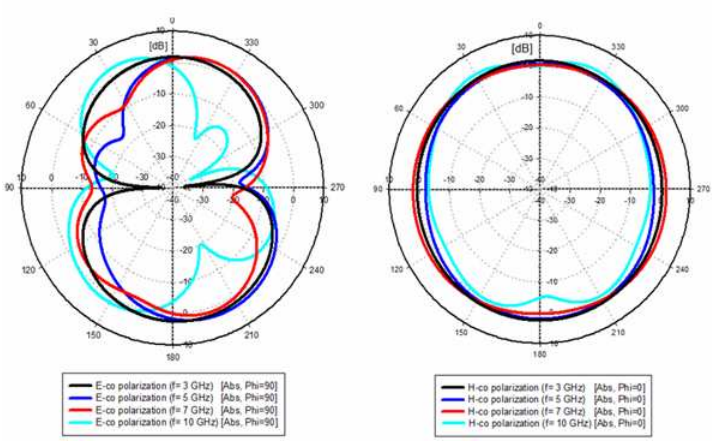

Figure 13. Antenna #1 simulated radiation pattern results for E-plane and H-plane in the frequency range between 3 GHz and 10 GHz.

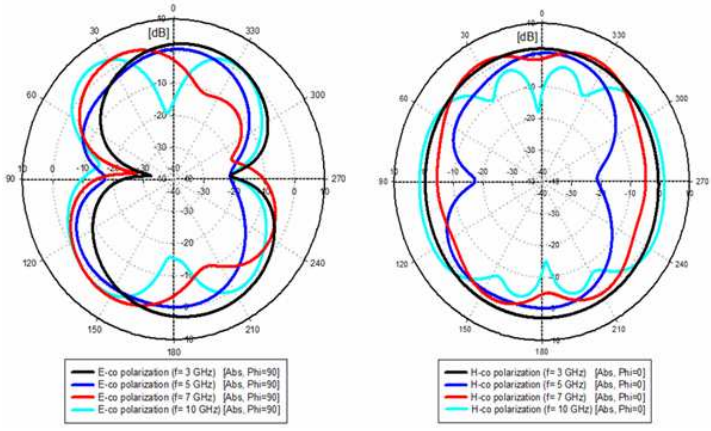

Figure 14. Antenna #2 simulated radiation pattern results for E-plane and H-plane in the frequency range between 3 GHz and 10 GHz.

power radiated was found to be at the side of the antenna. At 10 GHz most of the power radiated was at the top of the antenna.

5.3.3. Antenna #3 Polar Plot of Simulation Results

However, Figure 15 clarifies the behavior of 2D radiation pattern of E-plane and H-plane of antenna #3 design in the range of frequencies between 3 GHz and 10 GHz. The range of frequencies between 3 GHz

and 5 GHz found to have most of signal intensity at the bottom of the antenna, while most of power radiated at the bottom and side of the antenna in the range of frequencies between 6 GHz and 9 GHz. At 10 GHz, most of the power radiated at the top of the antenna but it also has many side lobes.

5.3.4. Antenna #1 Measured Results

Figure 16 below illustrates a snapshot of radiation pattern measurement setup inside an anechoic chamber, while Figure 17 shows the measured radiation pattern results for antenna #1 design at 3 GHz, 5 GH, 7 GHz, and 10 GHz. It can be seen from Figure 17 that antenna

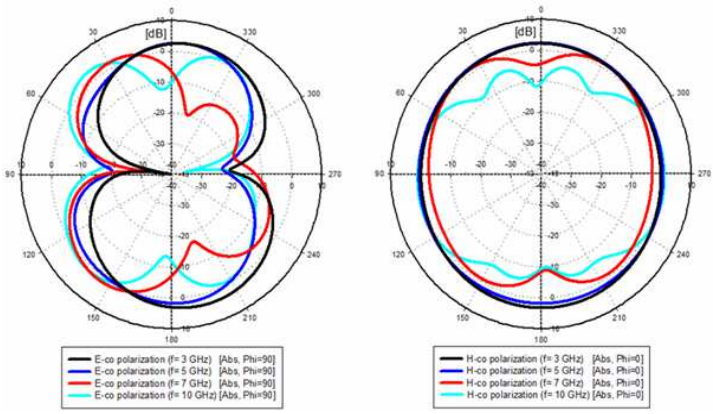

Figure 15. Antenna #3 simulated radiation pattern results for *E*-plane and *H*-plane in the frequency range between 3 GHz and 10 GHz.

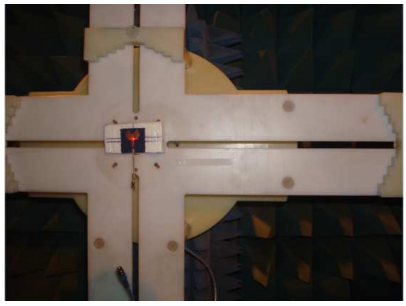

Figure 16. Snapshot of radiation pattern measurement setup inside an anechoic chamber for antenna #1 design.

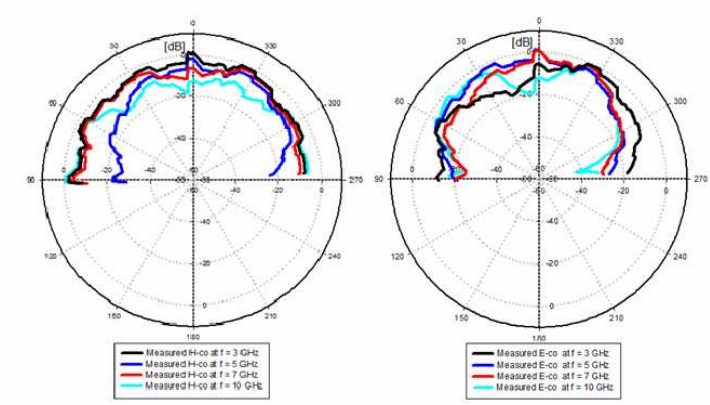

Figure 17. Antenna #1 measured radiation pattern results for E-co and H-co at 3 GHz, 5 GHz, 7 GHz, and 10 GHz.

#1 has good omni-directional radiation pattern in H-plane. However, in E-plane, the radiation pattern of the antenna is a kind of monopole-like shape.

Due to limitation of measurement equipments, the radiation patterns were plotted in the range between -90° and $+90^\circ$. In addition, the magnitude of the radiation pattern has been normalized to simplify the viewing of measured results. However, one can observe that there was a slight difference between simulated and measured radiation pattern results for both E-co polarization and H-co polarization of antenna #1 design. This slight difference can be related to fabrication tolerance and misalignment during measurement setup. However, both results correlate well to each other since the patterns were similar.

In contrast, simulated and measured radiation patterns on air for the button antenna reported in [1] showed good Omni-directionality with gain results of 2.6 dBi at 3.5 GHz, 1.9 dBi at 6 GHz and 3.4 dBi at 9 GHz [1].

5.4. Simulated Gain Results

5.4.1. Gain Results of Antenna #1

On the other hand, the variations of gain as functions of frequency of antenna #1 design were all demonstrated in Table 3. The lowest gain is 2.8 dB in the range of frequencies between 6 GHz and 8 GHz, while the largest gain is 4.1 dB at 10 GHz. The highest antenna efficiency was approximately 95%, which could be considered as a great value since

most of the commercial antennas had achieved efficiency between 50% and 60%. Results showed that the gain at frequencies range between 3 GHz and 10 GHz is less than 5 dB which denoted that antenna #1 design consumes low power. Moreover, the efficiency of the antenna also could be considered great since it is greater than commercial antennas.

5.4.2. Gain Results of Antenna #2

Table 3 demonstrates the variations of frequencies versus the gain of antenna #2 design. Maximum gain for this antenna was about 4.3 dB at 13 GHz while the minimum gain was about 2.0 dB at 4 GHz. The greatest percentage of efficiency is 98% which is at 6 GHz while the lowest efficiency was about 86% at 13 GHz. According to these results, antenna #2 design was found to be the low power and high efficiency antenna design among other designs in this paper.

Table 3. Gain and efficiency simulated results for Antenna #1, Antenna #2, and Antenna #3 designs.

Frequency [GHz]	Antenna #1		Antenna #2		Antenna #3	
	Gain [dB]	Efficiency [%]	Gain [dB]	Efficiency [%]	Gain [dB]	Efficiency [%]
2	-	-	-	-	2.6	92
3	2.6	93	3.3	93	3.6	93
4	3.6	93	2.0	90	3.0	93
5	3.2	93	3.4	92	2.8	94
6	2.8	95	3.4	98	3.4	95
7	2.8	92	3.8	93	4.2	94
8	2.8	95	3.9	92	4.0	92
9	3.7	98	4.2	92	4.2	95
10	4.1	93	4.2	95	4.9	91
11	4.0	88	3.6	95	4.3	89
12	3.8	85	3.8	90	3.9	91
13	-	-	4.3	86	4.0	92
14	-	-	-	-	4.0	91
15	-	-	-	-	3.9	85

5.4.3. Gain Results of Antenna #3

In opposition, the variations of frequencies versus the gain of antenna #3 design were all demonstrated in Table 3. The maximum gain achieved by antenna #3 was about 4.9 dB at 10 GHz. In contrast, the highest percentage of efficiency of antenna #3 reached 95% at two frequencies, 6 GHz as well as 9 GHz. However, the lowest efficiency was about 85% at 15 GHz. Consequently, results showed that antenna #3 design has low power consumption than other designs presented in this manuscript due to the achievement of gain results that was less than 5 dB in the wide range of frequencies between 2 GHz and 15 GHz. In addition, the efficiency of the antenna could be considered vast compared to commercial antennas.

Yet, all three-antenna designs that have been presented in this manuscript were intended to be mounted on a textile jacket with a specific separation from the human body. Investigation provided in this manuscript has proven that all three designs can be considered as successful designs using wearable materials. However, several wearable antenna design aspects that has been discussed in previous sections of this manuscript such as the specific separation from the human body, antenna bending, etc., need to be considered when designing such wearable systems. Therefore, those effects are currently under investigation. In addition, future work will also address the degradation on those antennas performances due to the presence of human body near the wearable antennas as well as evaluating the effects of interaction between wearable antennas and the user.

6. CONCLUSION

UWB wearable textile antennas with three different designs were presented in this paper. Generally, all three designs consist of a partial ground plane, modified circular patch with jeans substrate textile material that made those antenna designs suitable for wearable applications. A second layer of jeans textile material was placed on the top of the microstrip feed line to hide the feeding on the clothing. All three-antenna designs were successfully designed, constructed, and measured. The simulated and measured results showed that the proposed antennas have ($|S_{11}| \leq 10$ dB) at UWB frequency ranges, constant gain, high efficiency and stable radiation pattern over its whole frequency band. In addition, the compact size of the antenna further confirms its suitability for portable UWB devices.

REFERENCES

1. Sanz-Izquierdo, B., J. C. Batchelor, and M. I. Sobhy, "Compact UWB wearable button antenna," *Antennas and Propagation Conference*, 2–3, Loughborough, UK, Apr. 2007.
2. Sankaralingam, S. and B. Gupta, "Development of textile antennas for body wearable applications and investigations on their performance under bent conditions," *Progress In Electromagnetics Research B*, Vol. 22, 53–71, 2010.
3. Januszkiewicz, L., S. Hausman, and T. Kacprzak, "Textile body-worn exponentially tapered vee antenna," *IET Electronics Letters*, Vol. 42, No. 3, Mar. 2, 2007.
4. Chen, D. and C.-H. Cheng, "A novel compact ultra-wideband (UWB) wide slot antenna with via holes," *Progress In Electromagnetics Research*, Vol. 94, 343–349, 2009.
5. Barbarino, S. and F. Consoli, "UWB circular slot antenna provided with an inverted-L notch filter for the 5 GHz WLAN band," *Progress In Electromagnetics Research*, Vol. 104, 1–13, 2010.
6. Chamaani, S., M. S. Abrishamian, and S. A. Mirtaheri, "Multi-objective optimization of UWB monopole antenna," *Progress In Electromagnetics Research C*, Vol. 8, 83–94, 2009.
7. Gao, G.-P., Z.-L. Mei, and B.-N. Li, "Novel circular slot UWB antenna with dual band-notched characteristic," *Progress In Electromagnetics Research C*, Vol. 15, 49–63, 2010.
8. Ghazi, A., M. N. Azarmanesh, and M. Ojaroudi, "Multi-resonance square monopole antenna for ultra-wideband applications," *Progress In Electromagnetics Research C*, Vol. 14, 103–113, 2010.
9. Amini, F., M. N. Azarmanesh, and M. Ojaroudi, "Small semi-circle-like slot antenna for ultra-wideband applications," *Progress In Electromagnetics Research C*, Vol. 13, 149–158, 2010.
10. Zhang, X., Y.-Y. Xia, J. Chen, and W.-T. Li, "Compact microstrip-FED antenna for ultra-wideband applications," *Progress In Electromagnetics Research Letters*, Vol. 6, 11–16, 2009.
11. Klemm, M. and G. Troester, "Textile UWB antennas for wireless body area networks," *IEEE Transactions on Antennas and Propagation*, Vol. 54, No. 11, Nov. 2006.
12. Zhu, S. and R. J. Langley, "Dual band wearable antennas over EBG substrate," *IET Electronics Letters*, Vol. 43, No. 3, 141–143, Feb. 2007.
13. Winterhalter, C. A., J. Teverovsky, W. Horowitz, V. Sharma,

and K. Lee, "Wearable electro-textiles for battlefield awareness," *Mechanical Testing of Electro-textile Cables and Connectors*, Shur, Wilson, Urban, Ed., Materials Research Society, Warrendale, PA, 2003.

14. Van Langenhove, L., *Smart Textiles for Medicine and Healthcare*, CRC Press, Cambridge, England, 2007.
15. Tronquo, A., et al., "Robust planar textile antenna for wireless body lans operating in 2.45 GHz ISM band," *Electronic Letters*, Vol. 42, No. 3, Feb. 2, 2006.
16. Negookar, F., *Ultra-wideband Communications: Fundamentals and Applications*, Prentice Hall, Aug. 2005.
17. Eldek, A. A., "Numerical analysis of a small ultra wideband microstrip-FED tap monopole antenna," *Progress In Electromagnetics Research*, Vol. 65, 59–69, 2006.
18. Rahayu, Y., et al., "Slotted ultra wideband antenna for bandwidth enhancement," *Loughborough Antennas & Propagation Conference*, Loughborough, UK, Mar. 17–18, 2008.
19. Balanis, C. A., *Antenna Theory: Analysis and Design*, John Wiley and Sons, New York, 2004.